A LiDAR-based assessment of riparian zones for the Skagit River (WA) watershed

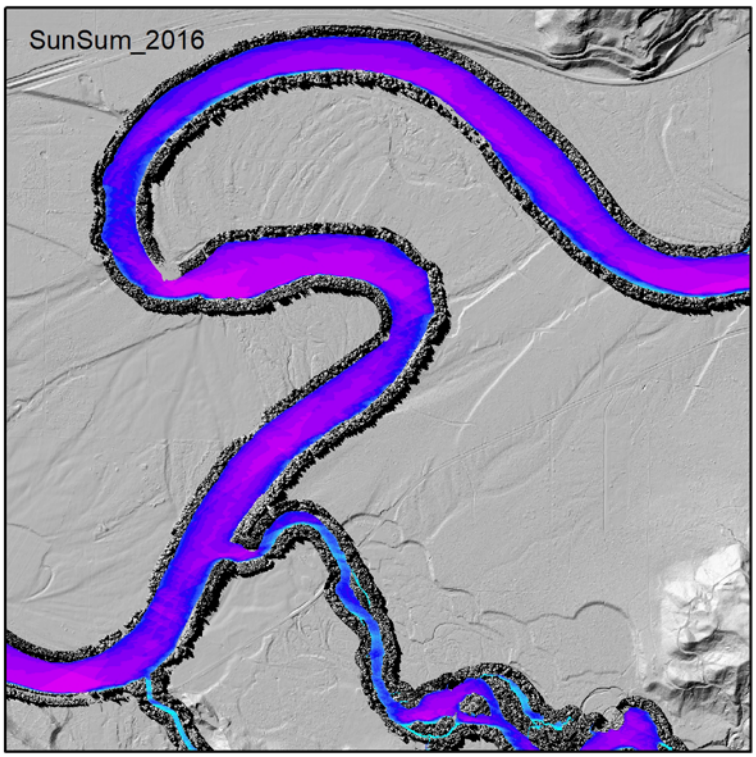

Tim Hyatt
Skagit River System Cooperative
February 25, 2021

Skagit River System Cooperative

Introduction

In the Skagit River watershed, as with most watersheds in the Pacific Northwest, it has been known for some time that the quality and extent of riparian forests is a primary driver of population dynamics for salmon and trout, including several threatened and endangered species (Hall et al. 2018, Quinn et al. 2018, SRSC and WDFW 2005). Skagit steelhead, for instance, despite the myriad freshwater and marine influences, exhibit density-dependent population characteristics that indicate juvenile rearing habitat as a predominant limitation on adult spawner returns (Scheuerell et al. 2020). Riparian forests affect that freshwater habitat in a number of ways: by shading and cooling streams, by providing large wood that creates pools and other habitat features, by stabilizing eroding banks, and by providing vegetative and macroinvertebrate inputs that drive the food chain, among other effects (Naiman et al. 2000).

Sun, shade, and temperature

The presence or absence of riparian vegetation can have pronounced temperature effects on rivers and streams (Seixas et al. 2018, Pollock et al. 2009, Brown and Krygier 1970). For a given rate of net solar input, the change in temperature of a stream is directly proportional to surface area and inversely proportional to discharge (Beschta et al. 1987, Brown 1969). Often the highest solar input and the lowest discharges occur simultaneously. Brown (1969) was among the first to model stream temperature energy balances in Pacific Northwest forested streams, taking into account solar radiation, evaporation, conduction, convection, and advection. Measured stream temperature values were within 1 F of the modeled value more than 90% of the time. Net thermal (solar) radiation was the predominant source of energy to these small Oregon streams, with evaporation and convection accounting for less than 10% of the total energy exchange (Brown 1969).

Streams fed by groundwater often display a more uniform temperature, both diurnally and year round (Johnson 2004). Poole and Berman (2001) point out the importance of hyporheic flow in regulating stream temperatures. Johnson (2004) showed that diurnal fluctuations of stream temperature in a bedrock reach were much greater than downstream in an alluvial reach, although mean daily temperatures were similar. Johnson's heat budget calculations showed that streams do not absorb large amounts of heat from the air, but that air and water temperature respond to the same temporal fluctuations in solar inputs. In a study of small streams near the limit of perennial flow, Janisch et al. (2012) found a clear difference in temperature response between intermittent streams with beds of coarse rock, as opposed to continuous streams with fine-textured stream beds and upstream wetlands. Small, intermittent streams where the water goes sub-surface were thermally unresponsive, due primarily to the interaction of groundwater and hyporheic flow (Janisch et al. 2012).

Peak daily temperatures are usually achieved during the late afternoon, and minimums just before dawn. Increased solar exposure not only leads to higher temperatures, but to

greater diurnal fluctuations (Kammer et al. 2020). In some unshaded situations the diurnal range in midsummer can increase by more than 15 ºC (Brown & Krygier 1970). Although heat exchange equations work well for short-to-medium reaches, on reaches longer than 1000 meters evaporative and conductive energy transfers begin to become significant dissipaters of heat and must be accounted for in the predictions (Beschta et al 1987). Likewise, streams exposed over long reaches will not continue heating indefinitely (Theurer et al. 1985). Because heat added to a stream is not readily dissipated, temperature increases in small headwater streams can cumulatively increase the temperature regimes of downstream reaches (Beschta and Taylor 1986).

The amount of shade or sun falling on a stream surface depends on several factors, such as the height and density of riparian forest stands, the width of riparian buffers, the width and orientation (azimuth) of the stream, and geographic shading from near or distant hills. The primary factor affecting shade is the height and density of riparian trees (Roon et al. 2021, Tompalski et al. 2017, Michez et al. 2013, Brown & Krygier 1970). On wide mainstem reaches the center of the channel is exposed to long hours of daylight, regardless of the size or density of the trees, and only the channel edges are affected by riparian shade. On small tributaries shade can come predominantly from understory vegetation (Brazier and Brown 1973, Schuett-Hames & Stewart 2019), which rebounds quickly after timber harvest. Vigorous riparian regrowth 30 years after harvest provided more shade than old-growth stands immediately upstream (Kaylor et al 2016). Pollock et al. (2009) found that riparian stand harvest in the prior 20 years had less effect on temperature than expected, due to rapid regrowth adjacent to the channel.

Brazier and Brown (1973) examined the importance of angular canopy density (ACD) in measuring stream shade. Their densiometer involved a sectioned mirror set near the stream surface to measure the portion of canopy blocking the sun at various angles of the summer day. They found an asymptotic relationship between buffer width and the energy hitting the stream, with a maximum ACD reached within about 80 feet, although 90% of that maximum ACD is reached within 55 feet (Brazier and Brown 1973). Steinblums et al (1984) measured angular canopy density at 40 sites in the Oregon Cascades, which ranged from and ACD of 15 to 84. Their plot showed ACD reaching an asymptote at about 80% shade between 80 and 100 feet buffer width.

Brown and Krygier (1970) measured summer stream temperatures before, during, and after experimental logging in streams along the Oregon Coast. Clear-cut streams showed distinct temperature increases the year after logging, but shade returned to the small streams in the second and third years. The summer maximum in the clear-cut stream rose 28 ºF over the prelogging maximum. The patch cut watershed had higher temperatures than the control stream both before and after logging, indicating that the patch-cut with a 100-foot buffer did not significantly alter temperature patterns in the adjacent stream.

Although direct mortality of fish due to temperature in Pacific Northwest headwaters is probably infrequent, temperature changes can influence rates of egg development, rearing success, species competition, and other factors affecting the population. Brett (1952) found that the range of greatest preference by all Pacific salmon species was from 12 to

14 ºC, with a definite avoidance of water over 15 ºC. In Ontario streams, Barton et al. (1985) found that maximum temperature appeared to be the most critical variable in determining suitability for trout. All streams with weekly maximum temperatures less than 22 C were inhabited by trout, whereas all streams with maximum temperatures above 22 C were marginal or without trout. Colder streams tended to have fewer fish species, and warmer streams had high concentrations of cyprinids (Barton et al. 1985). Reeves (1985) showed that the outcome of interactions between juvenile steelhead (age 1+) and the redside shiner (*Richardsonius balteatus*) was mediated by water temperatures. Trout dominated in cool water (12 to 15 ºC) and shiners dominated in warm water (19 to 22 ºC). Reeves (1985) also found that production of juvenile steelhead trout was 2.5 times greater in cooler water (12 to 15 ºC) than in warmer (19 to 25 ºC). Salmonids higher susceptibility to disease is brought on by a combination of higher metabolic rates and elevated levels of physiological stress (Beschta et al. 1987). Nakatani (1969) found that *columnaris* became well established in salmonids at temperatures of 17 to 18 ºC under crowded conditions, and when temperatures reached 21 ºC the disease killed most of the infected individuals. High temperatures can also have belated effects on marine survival. Holtby and Newcombe (1982), and Tschaplinski and Hartman (1983) showed that increases in late winter temperatures accelerated fry emergence. But the benefits of increased smolt size from higher temperatures, may be offset by increased saltwater mortality attributable to earlier migration (Beschta et al. 1987).

Large wood recruitment and source distance

As with temperature, large wood in streams has a profound effect on habitat suitability for anadromous salmon and trout (Quinn et al. 2020, Gregory et al 2003, Bilby & Bisson 1998, Bisson et al. 1987). Much of the research on large wood in streams has focused on channel and habitat forming processes (Collins et al. 2012, Czarnomski et al. 2008, Beechie & Sibley 1997, Abbe and Montgomery 1996, Montgomery et al. 1995, Robison & Beschta 1990, Bilby & Ward 1991, Swanson & Lienkaemper 1978), habitat benefits of large wood for salmonids (Penaluna et al. 2020, Roni & Quinn 2001, Rosenfeld et al. 2000, Fausch and Northcote 1992, Tschaplinski and Hartman 1983, Bustard and Narver 1975), and source distances of large wood recruited to streams.

Research on source distances for large wood shows a remarkable consistency, given the wide natural variation in types of riparian forests, methods of delivery, and geography. Source distance usually depends on the method of recruitment, whether windthrow, erosion, or landsliding. McDade et al. (1990) examined source distances at 39 sites in Oregon and Washington with mature or old growth stands. They found that 53% of the conifer pieces originated within 10 m of the stream, 70% of all wood originated within 20 m, and nearly 100% originated from within 50 m. The maximum observed source distance was 60.5 m. Van Sickle and Gregory 1990) used some of the same data as McDade et al. (1990) to model large wood recruitment, taking into account tree size, density, and fall probability. Their model demonstrated that trees entering from shorter distances contributed longer pieces with greater diameters, that nearly all pieces originated within 30 m of the channel edge, and 100% of pieces originated within 50 m. May and Gresswell (2003) compared wood delivery between small, steep colluvial

channels and larger alluvial channels. Colluvial channels received wood from farther upslope, as was also noted in McDade et al. (1990). Many of the smaller pieces had been moved and redeposited by the stream, but for those in alluvial channels where the origins could be identified, 80% originated from within 30 m of the channel. Murphy and Koski (1989) noted that windthrow and bank erosion were the most frequent delivery processes at work in Southeast Alaska streams, where landslide delivery accounted for only 4% of identified recruitment. They found that almost all (99%) of the identified sources of large wood were within 30 m of the stream bank (Murphy & Koski 1989). Working among old growth and second growth redwoods in northern California, Benda et al. (2002) found that over 90% of the wood enters the channel from within 30 m of the stream edge. In the absence of landsliding, in both old-growth and second-growth stands, wood recruitment originated from within 20 – 40 m of the stream. Landsliding caused recruitment distances to extend to over 60 meters (Benda et al. 2002). Johnston et al. (2011) found that erosion recruitment increased with increasing stream size, that wind-induced inputs accounted for 13% - 20% depending on channel type, and that wind recruitment increased in importance in the smaller channels. They found the distribution of source distances to be left skewed, with 90% of the large wood originating within 18 m of the stream in 90% of the cases. The maximum recruitment distance, like with McDade et al. (1990) and Benda et al. (2002), was 65 m. Source distance increased with increasing maximum tree height (Johnston et al. 2011).

LiDAR for environmental analysis

This paper uses an amalgamation of mostly high-resolution LiDAR to estimate shade and large wood contribution to streams. LiDAR has for decades been used as a highly accurate and adaptable data source for studies involving ground topography, vegetation height, forest canopy structure, leaf area index, biomass, forest fire fuels, and canopy gaps (Lefsky et al., 2002). Means et al. (2000) provided an early comparison of LiDAR and field techniques to measure tree height, canopy cover, and basal area in a variety of forests in western Oregon and Washington. Their regressions of LiDAR and field data resulted in r^2 values greater than 0.9 in every case, demonstrating that LiDAR measurements of tree height and other characteristics are sufficiently accurate for most forest research and assessment work. Andersen et al. (2006) rigorously measured the heights of trees using surveying instruments and compared actual heights to LiDAR measured heights. Working on Douglas fir and Ponderosa pine in western Washington, they found that LiDAR generally (for both species combined) underestimated height by less than a meter (73 cm , SD +/- 0.42 m). Wasser et al.. (2013) examined the accuracy of measuring riparian forest canopy height and crown density using both leaf-on and leaf-off LiDAR. They found that the 70^{th} percentile height value of LiDAR point clouds closely related to field measured values ($r^2 = 0.90$). Canopy height rasters (CHMs) that used an inverse distance weighted (IDW) construction were inferior to CHMs that used a maximum return elevation (Wasser et al. 2013). LiDAR methods tend to overestimate canopy cover, but are nevertheless more accurate than spectral (i.e. air photo) methods (Wasser et al. 2015). Hofle et al. (2009) developed an accurate and innovative method to delineate water bodies from landforms using LiDAR point clouds and the intensity signals associated with each return. By comparing the LiDAR derived water boundary to

RTK GPS measurements, Hofle et al. (2009) reported an average horizontal difference of 0.36m (with an RMSE of 0.45m). In a study from northern Vancouver Island, Tompalski et. al. (2017) used LiDAR to examine stream characteristics such as stream gradient, width, canopy cover, and shade. Tompalski et al. (2017) found that the LiDAR derived stream network was highly detailed, and provided valuable information for improved forest and resource planning, offering objectivity and consistency over large areas.

In this paper an amalgamation of high-resolution LiDAR data sets are combined to examine the height and location of riparian stands, the shade cast by those stands on the rivers and streams, and the potential for large wood contribution from those riparian areas. In order to accurately predict riparian interactions, the basin hydrography was generated from LiDAR, with supervised editing based on air photo interpretation and field checks. Open water polygons were generated from LiDAR-derived channel edges, and widths of single-thread streams were modeled from basin parameters. Once the edges of the riparian zones were known, 300-foot buffers were used to extract the vegetation height along all anadromous reaches, and the shade and large wood contributions from those buffers were analyzed in aggregate, by land use, and compared to site-potential stands. Unlike other studies [cite], there was no attempt to delineate individual riparian trees, to predict which trees would likely fall toward the stream, or to estimate the stored volume of large wood in the streams. Nor was there an effort to model stream temperatures. Those studies will be forthcoming. In the interest of guiding restoration and protection efforts, this study examines precisely which riparian zones do or do not have the potential for contributing large wood, which stands are currently providing shade, and where planting and other stand improvements will provide the most shade benefit in the shortest time.

Methods

High-resolution LiDAR rasters (Table 1) were assembled for the entire Skagit anadromous zone and converted to common horizontal (State Plane Washington North NAD83, ft) and vertical (NAVD88, ft) spatial reference frames. To calculate consistent watershed areas throughout, areas of the Skagit watershed without LiDAR were represented by a USGS 10m DEM, and merged with the high-resolution LiDAR on a 3-foot grid spacing.

Table 1. LiDAR flight characteristics

LiDAR flight	Acquisition Year	Source/Client	First return point density (pt/m^2)	Ground Classified (pt/m^2)
USGS 3DEP	2016 - 2017	USGS, WaDNR	12.29	2.46
Glacier Peak	2014-2015	USGS Volcano Observatory	27.05	2.86
Mt Baker	2015	USGS Volcano Observatory	19.73	2.34
Skagit Coastal*	2019	NOAA	14.92	8.94
2006 Whatcom-Skagit	2006	USGS	~0.5**	

* Water-only tiles omitted from density calculations

**PD= 1/point spacing^2. this is the nominal contract spacing, not the final measured

New hydrography for the Skagit and Samish watersheds (WRIAs 3 & 4) were generated using the combined LiDAR and 10m DEM mosaic. Channel initiation was set to 25.46 acres, which approximates hydrography on the USGS 7.5 minute topographic maps. Single thread hydrography was generated in ArcGIS (Environmental Systems Research Institute) using standard tools for flow direction, filling sinks, and flow accumulation. Extensive editing of the underlying DEM was necessary to direct flow correctly through natural and anthropogenic modifications such as road culverts, dams, ditches, and other flow obstructions. Manual editing was also necessary at lakes, ponds, wetlands, floodplains, and other closed depressional areas to correctly align single-thread hydrography to known routes visible on aerial photographs and in the field. Single thread hydrography was attributed to include, channel slope and basin area, among other characteristics. Stream widths were calculated for each reach based on Hyatt et al. (2004). A geometric stream network was combined with known upper limits of fish distribution to extract stream reaches accessible to anadromous salmonids.

Mainstem and large tributary channel polygons were generated to delineate the edge of the riparian zone, either where the edge of the active channel meets a channel embankment or where the channel meets riparian vegetation taller than 12 feet. Channel contours were generated using a relative elevation model (REM) depicting the elevation of floodplain features relative to the minimum elevation locally within the river channel, which removes the longitudinal channel slope. By removing the channel slope from a DEM, REMs exhibit side channels, sloughs, and floodplain boundaries more clearly than in elevation DEMs, and contours from REMs are readily assembled to delineate a channel boundary approximating the bankfull width. River REMs were used to delineate channel islands, and similar upland REMs were generated to delineate lake, pond, and wetland boundaries where those ponds and wetlands were aligned along anadromous streams. Channel polygons minus channel islands, plus lakes, ponds, and adjacent wetlands, plus modeled widths along single thread streams, were merged into an “open water” polygon for riparian analysis.

To examine shade effects from riparian zones (and excluding trees on adjacent uplands), a 150-foot full-canopy (all return) riparian buffer was generated along the open water and channel island polygons, and around the anadromous reaches of the single thread hydrography. Within the buffer polygon the heights of vegetation were added to a bare-earth DEM to create a forested buffer zone along all anadromous water bodies (accessible rivers, streams, lakes, ponds, and wetlands) including the edges of channel islands (Figure 1). Outside the buffer zone, and within the open water polygons, the riparian DEM reverts to bare earth.

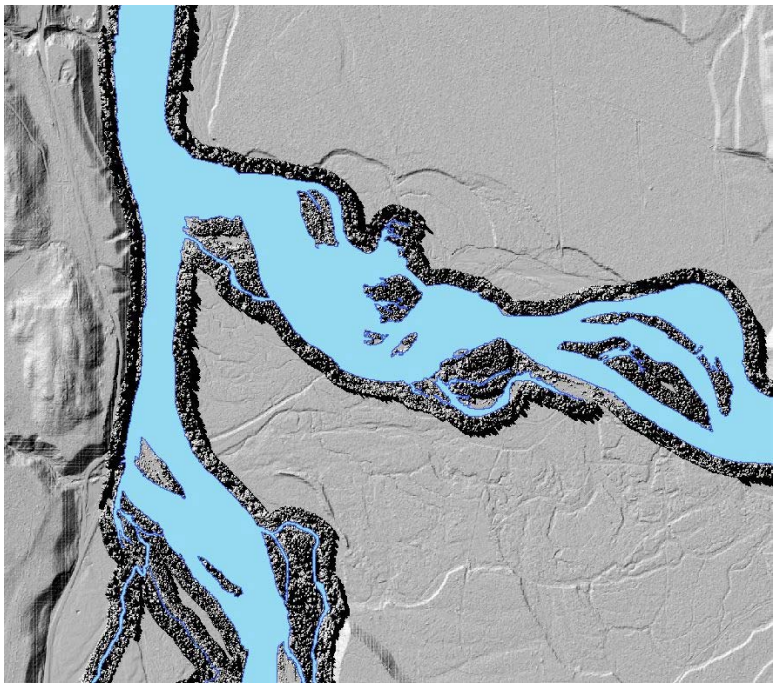

Figure 1. Hillshade image of 150-foot full-canopy buffer combined with bare earth elevations beyond the buffer extent. Canopy buffer was used to calculate stream shade as well as large wood recruitment potential from riparian zones. Area shown is the confluence of the Sauk and Suiattle rivers.

Similar to the current conditions riparian DEM, a comparison DEM was generated to depict site potential tree height (SPTH) along study area rivers and streams. The Washington Department of Natural Resources (DNR) digital site index maps were edited to correspond to new river locations due to channel migration. Tree height was determined for each map polygon using the DNR 100-year site index. Site indexes were used to generate a SPTH DEM within the same 150 foot buffer as the current condition LiDAR riparian DEM. However, the DNR site index maps, and therefore the SPTH input rasters, do not cover federal lands and do not have the same extent as the LiDAR derived input rasters. The Sauk River above Darrington and other important anadromous reaches (e.g. upper Illabot Creek and upper Cascade River) were necessarily excluded from the SPTH comparisons.

Sun azimuth and altitude, obtained from the National Research Council of Canada, were used to model shade that would be cast by the riparian DEM for each hour of the day on the longest day of the year (June 21). The rasters for each hour were then summed to depict the number of hours of sun falling on each open water (3x3 ft) cell, over the entire watershed. The same routine was also run using the SPTH DEM, and the results of the current (2016) conditions were clipped to the extent of the SPTH raster for comparison.

The accuracy of the shade DEM was evaluated by field measuring on-the-ground shade boundaries with a map-grade geographical positioning system (Trimble Geo XT) in late June. Shade boundaries from the DEM model were converted to polylines, and the

distance of each GPS node to the shade boundary was measured with the ArcGIS GenerateNearTable function.

To evaluate the potential contribution of large wood to streams, the height of each 3-foot cell in the riparian DEM was divided by the distance of that cell to the channel edge. The resulting height/distance (h/d) ratio was used as a surrogate for which cells, and thus what proportion of the riparian zone, would be capable of contributing large wood to the stream if the tree were to fall directly toward the stream. Cells with a height/distance ratio of <= 1 would not currently be capable of contributing wood– absent gravitational sliding of the tree or channel migration toward it. Pixels with a height/distance ratio of > 1 were considered functioning in terms of wood recruitment, and pixels with h/d ratios of >2 were evaluated for potential wood contributions to the stream.

Results

Shade potential

The accuracy of LiDAR in estimating tree heights has been reported extensively in the literature (Wasser et al. 2015, Wasser et al. 2013, Anderson et al. 2006, Lefsky et al. 2002, among many others) but the accuracy of shade projection generally has not. Test plot shade rasters, encompassing fixed structures as well as trees (Figure 2), were generated from the sun angles described in the methods section, and compared to GPS field measures of shade lines. Despite some GPS multipath reflections from the barns, average distance of shade points to the shade raster line was 3.11 feet (RMSE 4.08), which is slightly greater than the dimensions of the raster pixels used in the shade models.

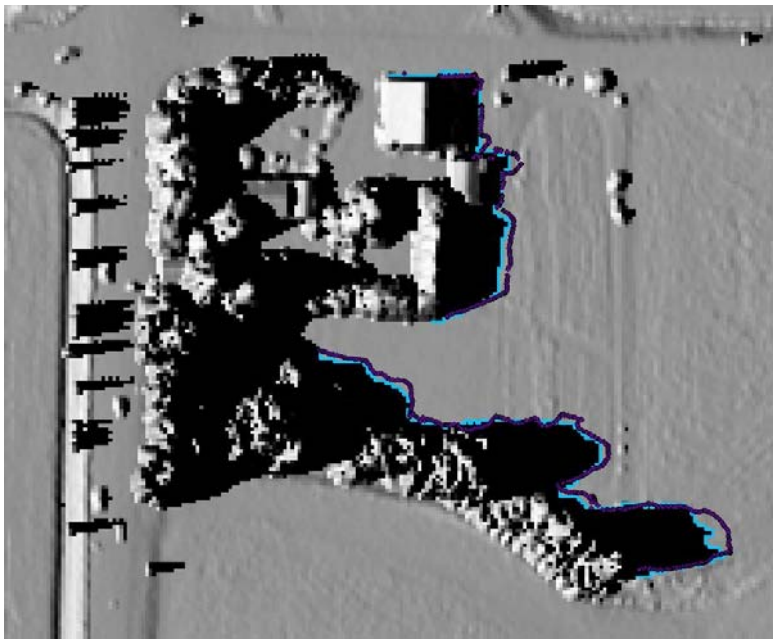

Figure 2. Shade test plot comparing the shade raster edge (blue line) to GPS points in late June (purple). Average distance from

GPS points to shade line was 3.11 feet (RMSE 4.08). GPS points were collected four years after the LiDAR flight, which partially explains the discrepancy on the taller trees.

Comparisons between the (2016) current riparian conditions and the SPTH modeled conditions were limited to the area covered by the DNR site class data, which excludes Federal lands. The areas without site class data (and therefore SPTH estimates) are in National Forests and National Parks, predominantly in the upper reaches of the Baker, Sauk, and Suiattle rivers, and Illabot, Jackman, and several smaller creeks. As expected, most of the channel area exposed to direct sunlight throughout the day was on the wider Skagit and Sauk River mainstem channels. On a hypothetical (i.e. no clouds) June 21st, under current (2016) conditions, over 81 percent of the channel area is exposed to eight hours or more of direct sun (Figure 3). Under the SPTH scenario that portion falls to 67 percent. The SPTH scenario shows a greater proportion of the channel receiving 0-10 hours of sun, and a smaller proportion receiving 11-16 hours of sun. Overall, on mainstem and tributary channels on non-Federal lands, the SPTH scenario provides 18% more riparian shade than the 2016 actual conditions.

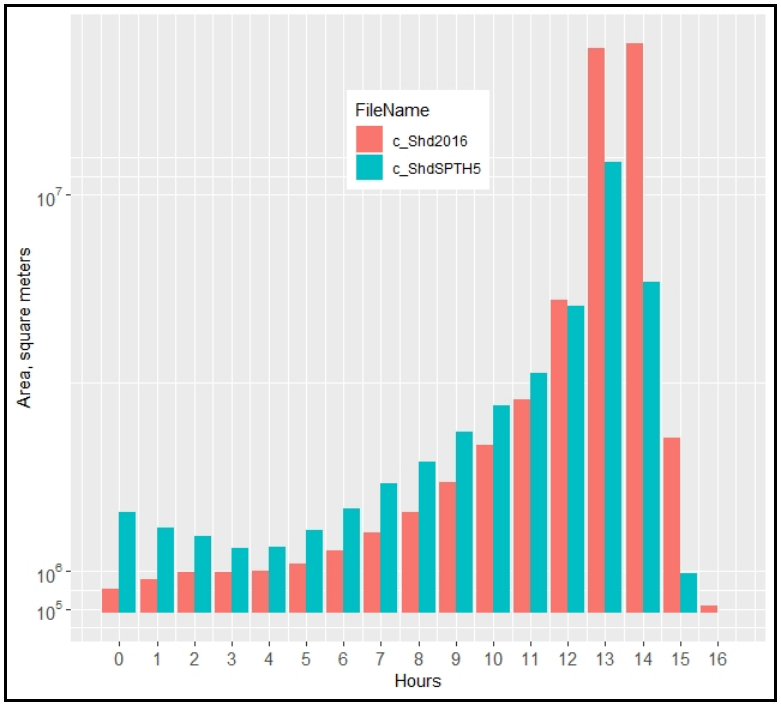

Figure 3. Comparison of the area of sunlight on the open channel in 2016 with the modeled SPTH scenario. The SPTH scenario had more areas exposed to only a few hours of sunlight, and fewer areas exposed to more than 10 hours of direct sun.

Direct solar insolation on water surfaces is at a minimum early and late in the day, and reaches a maximum around noon. Heat intensity from sunlight is likewise highest at mid-day, as the solar rays have less atmosphere to penetrate and the angle of incidence is closer to 90 degrees. The 2016 LiDAR coincides with a 2006 LiDAR flight along the

Skagit mainstem and several major tributaries, but the 2006 data excludes most of the Baker, Sauk, and Suiattle rivers. Figure 4 compares the direct solar insolation between 2006 and 2016, and from the SPTH scenario, for the area common to all three data sets. At noon on a hypothetical June 21st, 94% of the channel is under full sun in 2016, compared to 96% in 2006. In the SPTH scenario solar insolation over the same reaches is 87%.

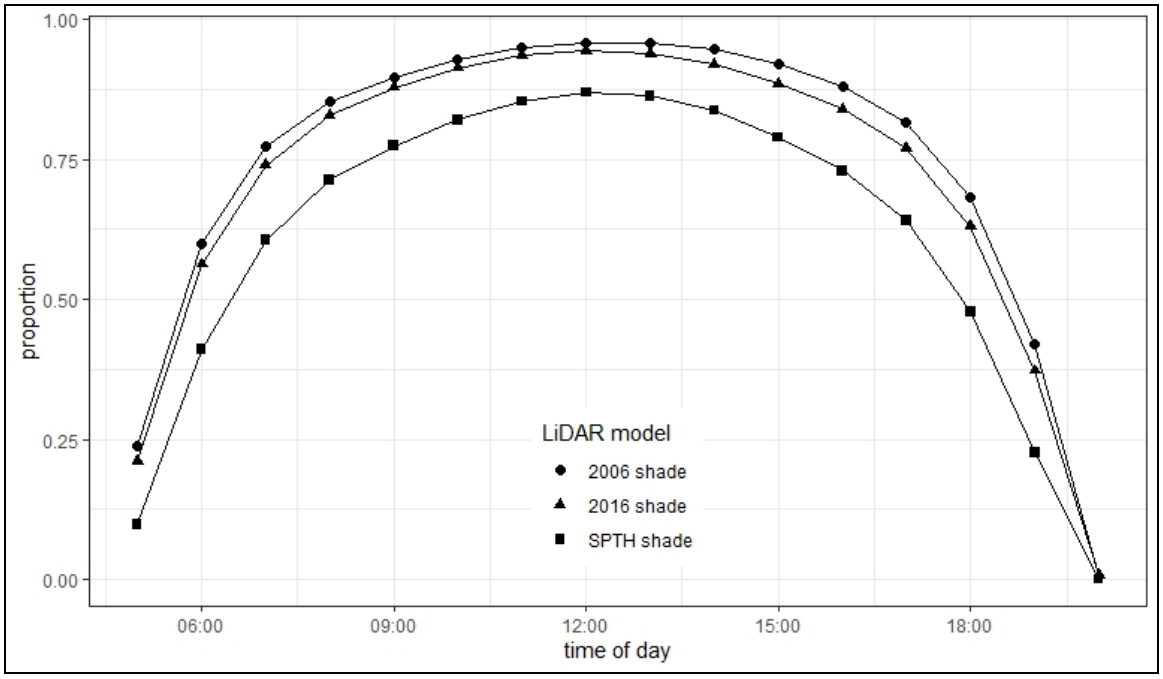

Figure 4. Proportion of the open channel subject to direct sun, for each daylight hour on a hypothetical June 21st. Plot is limited to areas common to the 2006 and 2016 LiDAR and to the SPTH data on non-Federal lands. Even in mid-day, the SPTH scenario provides 7% more shade at the channel margins than the current (2016) conditions.

The wider mainstems of the Skagit, Sauk, Suiattle, and Cascade are open to solar insolation even under the SPTH scenario. But the tributaries receive substantially more shade, both currently and with modeled SPTH riparian zones. This is true of both larger and smaller tributaries. Figure 5 compares the increased shading along anadromous tributaries, both currently and under the SPTH conditions. Figure 5 excludes mainstems on the Skagit, Sauk, Suiattle, Baker, and Cascade rivers, plus the larger lakes, ponds, and sloughs. Figure 5 is also limited to where the DNR site class polygons allow an estimation of SPTH, and so does not include federal lands. On anadromous tributaries the SPTH scenario results in less than 25% of the solar insolation modeled in the 2016 conditions. Given the narrower widths in the tributaries, the proportionally greater shade effect from reaching SPTH conditions could be reached in a shorter timespan than would be required to achieve the maximum shade benefit along the mainstems.

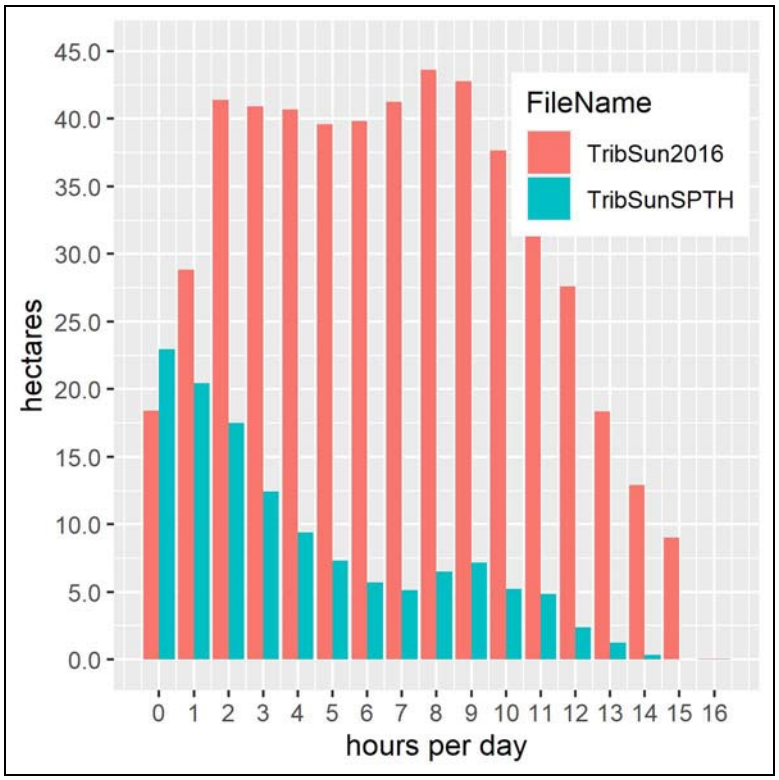

Figure 5. Comparison of current (2016) shade to SPTH shade in tributaries, in hours of sun on the channel on a hypothetical June 21st.

Large wood potential

Height-to-distance ratios were interpreted as a surrogate for wood contribution to streams, on the assumption that forest areas (represented by riparian pixels) with an h/d ratio less than 1 would not be capable of contributing large wood to the channel even if those trees were to fall directly toward the stream. Height/distance ratios of up to 8 were calculated within a 300 foot riparian buffer zone. Areas with an h/d ratio greater than 1 were considered functional for wood contribution, and h/d ratios greater than two were interpreted as capable of generating sizeable, functional wood to the stream.

Overall the height/distance ratio fell off rapidly with distance from the channel edge. Over the entire basin (including federal lands) more than 78% of riparian areas within a 300 foot buffer (and 61 percent within a 150 foot buffer) had an h/d ratio of less than 1, and would therefore not be considered “functional" regarding wood contribution. Within the 150 foot buffer 39% of riparian zones had an h/d ratio of 2 or greater (Figure 6). More than 98 percent of the currently functional wood grows within 150 feet of the channel edge. The HD8 category dominates the stands closest to the channel edge, but falls off rapidly within the innermost 30 feet of the riparian zone. The aggregated functional stands (HD2 through HD8) show a predictable and mostly linear decline in relative abundance from the channel edge out to about 150 feet. More than 45 percent of the

riparian zone within 30 feet has an h/d ratio of less than or equal to 1, indicating that substantial riparian areas adjacent to streams provide almost no wood or shade.

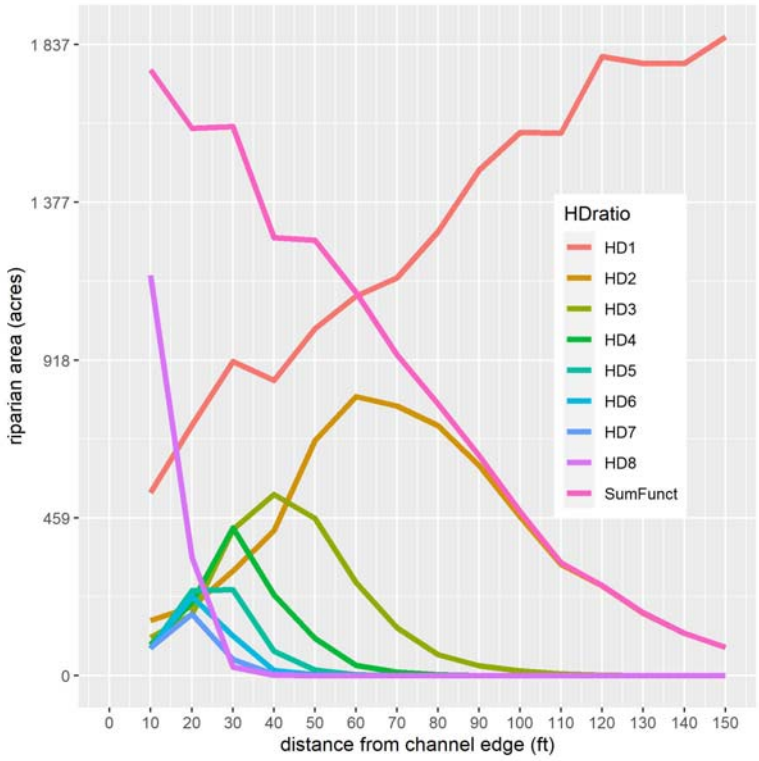

Figure 6. Height-to-distance ratio plotted against distance from the stream edge. The h/d ratio indicates the potential for a riparian stand to contribute large wood to the stream. Trees adjacent to the channel have an h/d ratio of 8 or greater, but that ratio falls off rapidly with distance from the stream. Most (91%) of the current wood recruitment potential is within 100 feet of the stream edge. The outer reaches of a 150-foot buffer are almost entirely incapable of contributing wood.

Riparian stands capable of delivering large wood to streams (HD2 through HD8) are far more abundant in federal, state, and commercial forests than in agricultural or rural residential zones, both by proportion and by total area (Figure 7). Within a 150 foot buffer, federal forests make up the largest total area (28%) of anadromous stream riparian zones in the Skagit watershed (including portions in Whatcom and Snohomish counties), followed by rural residential zones (25%), agriculture (21%) tied with commercial forests (21%), and urbanized areas (4%). Approximately 63% of functioning riparian zones (HD2 – HD8) are distributed among federal, state, and private forest zones. More than half (54%) of non-functional zones (HD1) are in the agricultural and rural residential zones. All zones have substantial portions of non-functional vegetation, primarily those furthest from stream edges. In areas zoned for forestry, HD1 areas are predominantly distant from the channel, and greater proportion of riparian zones are in functional (HD2 – HD8) categories, whereas in agricultural and rural residential zones the HD1 areas are

more often adjacent to the channel, and there are smaller functional areas, indicating greater recovery potential from restoration.

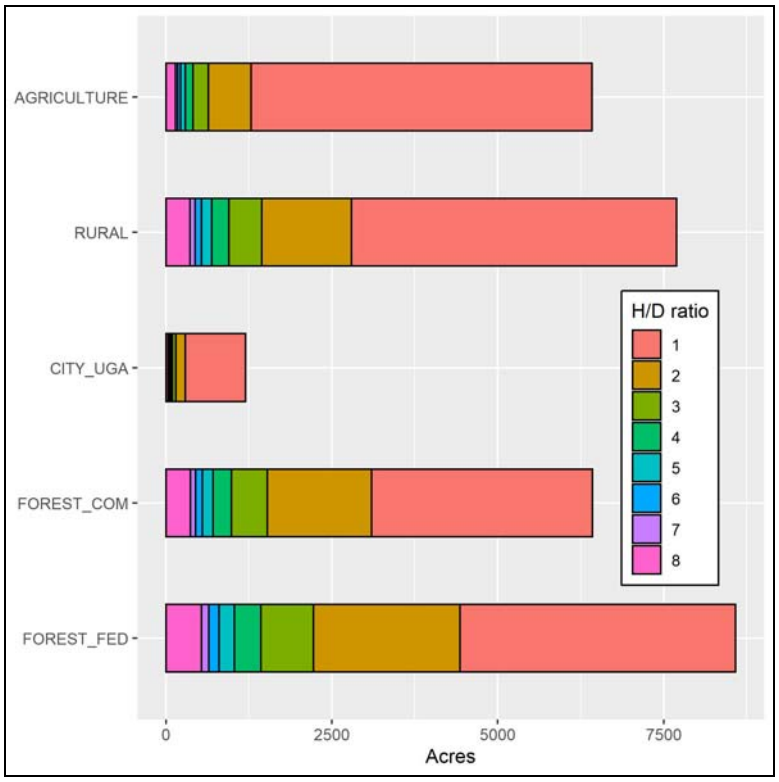

Figure 7 Acreage of riparian stands by height/distance ratio and land use. Commercial and federal forests have larger and proportionally more areas of functional riparian zones than in agriculture zones or urban growth areas.

Discussion

Several of the data sets described in this paper are both detailed and comprehensive, and are best utilized in a GIS. The shade maps in particular (Figure 8), which show the hours of sun and shade on each anadromous reach of the Skagit, provide comprehensive information to restoration practitioners for planning restoration, planting, and acquisition projects. Subtracting the hours of sun under current conditions from the modeled SPTH scenario shows precisely where riparian planting will create the most shade improvement over time. Although centerlines of most mainstem reaches will remain subject to full sun regardless of riparian conditions, the shade difference raster demonstrates that mainstem channel edges benefit, sometimes substantially, from taller trees in the riparian buffer. This improvement is depicted graphically in Figures 8? and 2?).

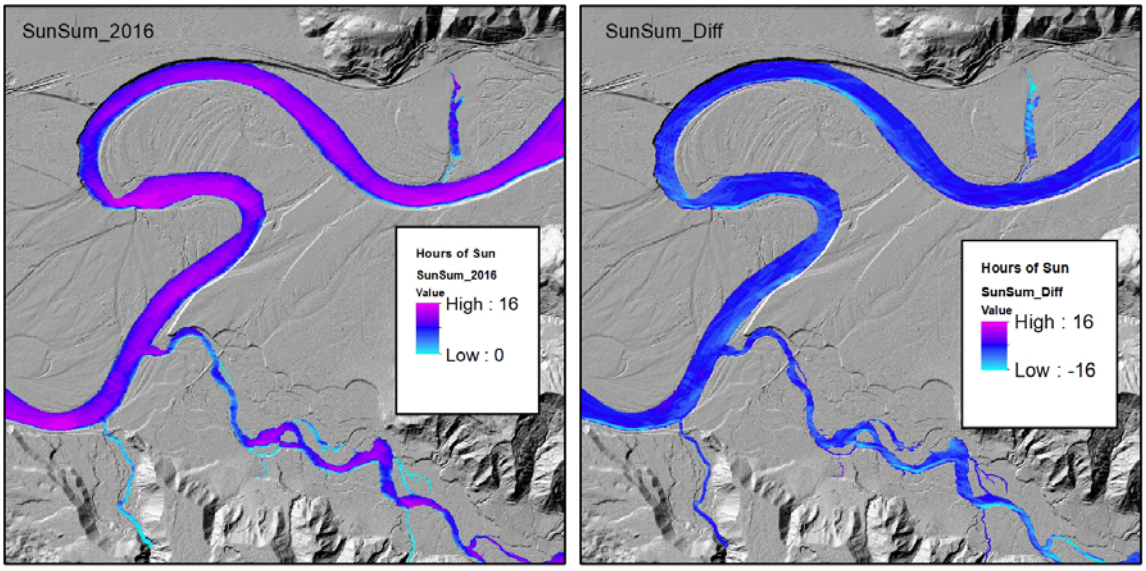

Figure 8. Shade maps of the Skagit mainstem and Finney Creek confluence. The greater hours of sun are more pronounced on wider channels and on east-west reaches. The difference between current conditions and the SPTH scenario is most pronounced on the south banks of both mainstems and tributaries.

Aerial photographs are frequently used for riparian and geomorphic analysis (Pierce et al. 2018, Fullerton et al. 2006, Hyatt et al. 2004, Poole et al. 2002, Lunetta et al. 1987) as they are ubiquitous, comprehensive, frequent, and relatively (compared to LiDAR) inexpensive. Air photos have the disadvantage of obscuring forested stream banks, and omitting the portions of stream channels that are usually shaded. The advantages of LiDAR are apparent in medium-to-large tributaries, where the stream edge is invisible. LiDAR excels in capturing the proportion of stream under shade, where aerial photos often indicate near or full canopy closure. LiDAR-derived channel boundaries that delineate both banks, as opposed to single-thread hydrography, identify the extent to which the wetted channel may be fully shaded by overhanging canopy. Figure 9 shows three depictions of a medium-sized tributary to the Skagit. Measured by the aerial photo tree cover and single-thread stream. The LiDAR canopy height (Figure 9a) shows the wetted stream channel of upper Day Creek in deep green, as does the air-photo derived tree canopy in Figure 9b (Pierce et al. 2020). But the stream channel is considerably wider when not obscured by tree canopies, as depicted in the bare-earth LiDAR hillshade in Figure 9c. Figure 9 demonstrates that measuring the riparian zone from the stream centerline significantly underestimates channel margins and therefore the extent of the riparian zone (magenta outlines). Riparian vegetation cover in the LiDAR model is 50% greater than in the air-photo estimate, due to the mis-alignment of where the riparian buffer begins. [work the Watershed Council work into this paragraph]

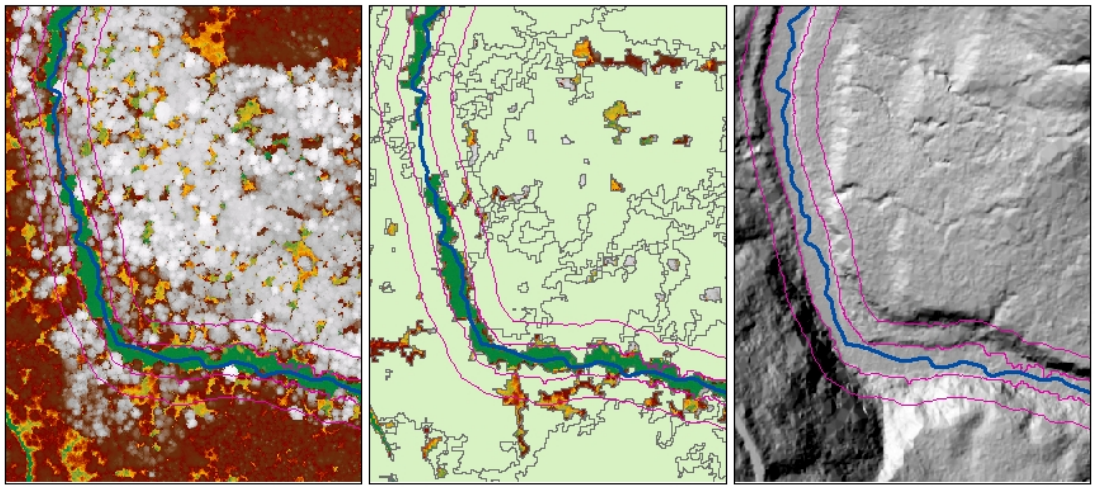

Figure 9. Three riparian depictions along a reach of upper Day Creek. Fig 9a (left) is the LiDAR tree height canopy, with the stream channel depicted in deep green. Fig 9b (center) is the same area with an overlay of tree height obtained from air photos (Pierce et al. 2020). Figure 9c (right) is a bare earth hillshade that reveals the true channel width. A 66-foot riparian buffer is shown as a magenta outline, and the NHD single thread hydrography is a dark blue line. The 66-foot buffer along the NHD thread is not shown. Within the respective 66-foot buffers, the air-photo tree canopy is 55.5% tall trees (> __ feet) and the LiDAR buffer is 83.6% tall trees.

One of the shortcomings of the raster-based shade model presented here is it's impenetrability to sun, that is, it presents the forested riparian stands as an opaque wall instead of a porous tree canopy. Riparian stands permit a varying amount of light to pass through, depending on forest type, stand density, and width. The ability of LiDAR to penetrate small canopy gaps allows for the modeling of shadows cast on the forest floor (Tompalski et al. 2017, Mücke et al. 2011), or streams, using LiDAR point clouds instead of rasters, as was done here. Unfortunately, most LiDAR data, as with the Skagit data, is collected in a leaf-off condition, which complicates or prevents an accurate estimate of the leaf area index (LAI), a common measure of the light blocked or absorbed by the forest canopy. A light penetration index (LPI), using the ratio of leaf-on LiDAR points that reach the ground to the total point returns, can accurately capture the direct solar radiation under a forest canopy (Bode et al. 2014). Fractional canopy cover can be estimated by leaf-off LiDAR, but the leaf-off canopy underestimates FCC by 19-24% (Wasser et al. 2013). Using LiDAR point clouds to model light penetration in riparian canopies is a promising avenue for estimating the width of riparian buffers necessary to effectively shade streams under a variety of stream and forest conditions, but leaf-on LiDAR in the Skagit is mostly lacking.

Although the LiDAR data sets for the Skagit were relatively large, the canopy height, distance, and shade data were relatively simple to extract once those rasters had been reprojected and assembled into a coherent basin-wide coverage. The more laborious tasks were correcting the single-thread hydrography for correct flow alignment, generating channel edges, and assembling those edges into channel polygons. Without accurate hydrography the edge of the riparian zone is unknown, the various data sets (between years, for instance) do not align, and model results are confounded by obvious spatial anomalies. Johansen et al. (2011) demonstrated an automated geographic object

extraction method using LiDAR terrain models and eCognition software to delineate stream channels and riparian zones. Tompalski et al. (2017) extracted single-thread hydrography using standard methods from commercial forest areas, and estimated shade cover, canopy height, stream slope, stream width, and potential fish distribution. Their stream width, as with Johansen (2011) and Michez et al. (2013), began with a rasterized stream centerline that is "grown" according to the relative elevation and adjacency of nearby DEM cells. In this Skagit work, streams in forested hillslopes were more easily modeled than those in the lowlands, where anthropogenic changes often require manually correcting streams, guided by a combination of field knowledge, LiDAR, and air photo interpretation. Automated methods of extracting stream polygons and delineating riparian edges, (as with Tompalski et al. 2017, Michez et al. 2013, and Johansen et al. 2011) would significantly reduce the data preparation effort and allow a more direct extraction of shade and wood potential from LiDAR.

The height/distance raster covers the same geography as the shade rasters, but is likely not as informative to restoration practitioners as the shade difference raster. The h/d raster shows a consistent pattern throughout the watershed– that trees close to the stream edge are capable of providing wood, but riparian stands at a distance typically are not (Figure 10). This pattern is more widespread in agricultural areas but also apparent in forested areas. Where trees are short or missing along the channel edge, that condition is also reflected in the shade raster. The advantages of planting or accelerating riparian growth is especially reflected in the difference between the SPTH shade raster and the current shade conditions. The shade difference map (Figure 10), for example, emphasizes the advantage of riparian improvement (planting) on south banks and narrower channels.

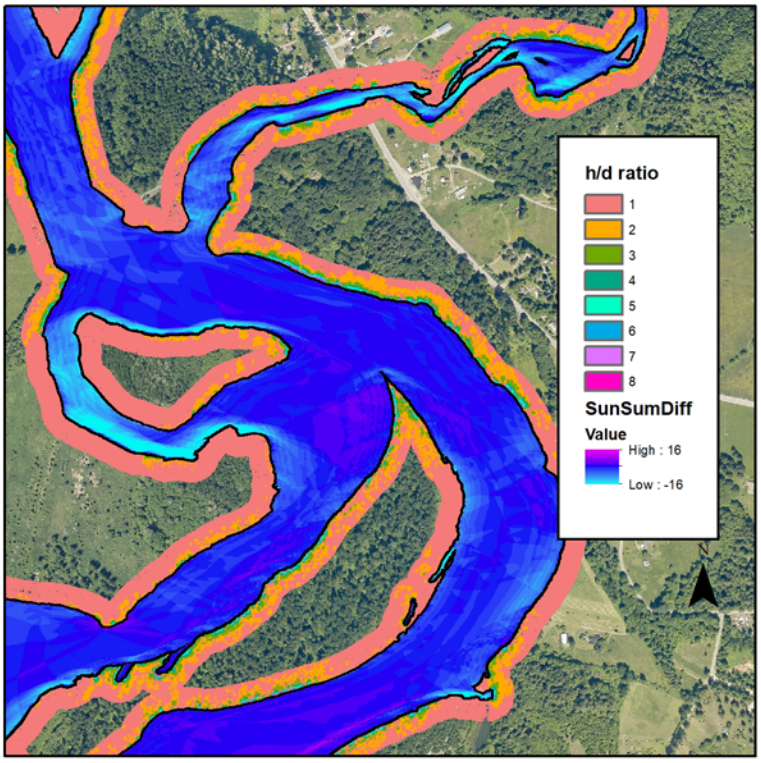

Figure 10. The h/d raster and the shade difference raster both show areas where riparian forests are lacking, but shade difference raster also shows where riparian improvements will have the greatest effect when the trees mature.

Height-to-distance ratios in the Skagit correlate well to large wood source distances reported elsewhere, considering most studies on source distance are from mature or old-growth forests, whereas the Skagit data is comprehensive over all anadromous river and tributary reaches. Whereas McDade reported 70% of large wood pieces (those for which the source could be identified) fell from within 20 m of the channel, the comparable number from the Skagit h/d ratio is 72%. Benda et al. (2002) confirm that wood recruited from old-growth and mature stands is larger than from the younger mixed stands found in most of the Skagit. The model constructed by Van Sickle and Gregory (1990) predicted ~90% of wood pieces originating from within 20 m of the stream. Murphy and Koski (1989) reported 95% of trees from within 20 m, but that 50% originated by bank erosion from within 1 m. Benda et al. (2002) likewise reported 90% of wood entering from within 30 m, and that bank erosion was responsible for greater than 50% of recruitment. Johnston et al. (2011) reported 90% of large wood from within 18 m of the channel in 90% of the sites. The Van Sickle and Gregory model predicted wood contribution from a variety of angles of tree fall, which would also be true of field studies. The h/d ratio by comparison implies wood contributions orthogonal to the bank (nearest distance). In the natural world, source distances depend in large part on the recruitment mechanism. The nearest trees are recruited by erosion, the furthest by landsliding (May and Gresswell 2003, Murphy & Koski 1989). May & Gresswell reported 80% of wood pieces in alluvial channels in the Oregon Cascades originated from within 30m of the channel. The

corresponding 30 m figure for Skagit h/d rations is 87%, including both alluvial and colluvial channels.

Conclusions

LiDAR provides data that are both detailed and comprehensive, and well suited for assessing riparian zone quality and extent over large areas and at a local site scale. Methods developed in this work correctly project shade from trees and structures with an accuracy commensurate with the resolution of the underlying raster data. Accurate LiDAR depiction of riparian interactions is predicated on an accurate delineation of streams and open-water areas. Because the Skagit mainstem is wide, more than 80% of the open channel is exposed to at least 8 hours of direct summer sunlight. Were the riparian zone comprised of trees meeting the site class (site potential tree height) threshold, that proportion drops to 67%, primarily along the mainstem channel margins and the tributaries. In the tributaries, excluding the mainstems, SPTH shade is approximately 25% of current (2016 LiDAR) conditions. The potential for large wood recruitment to streams is highest adjacent to the channel and drops off rapidly with distance from the stream. More than 98% of functional wood currently grows within 150 feet of the stream. Commercial and federal forests have a greater proportion of functional wood within the riparian zone. Agricultural and rural-residential areas have substantial proportion of non-functional riparian forests, particularly unforested areas immediately adjacent to salmon-bearing streams. Areas most in need of riparian restoration and protection are clearly identified in this method by examining the difference between current conditions and what would be achieved if riparian zones were at their site potential.

Acknowledgements

This work was supported by EPA grant PA00J99101 to the Swinomish Tribe. Thanks to Mike Maudlin, Victor Johnson, and Ann Stark at the Lummi Tribe for the initial (Nooksack River) shade model. Gerry Gabrisch at the Lummi Tribe and Tyson Waldo at the Northwest Indian Fisheries Commission contributed valuable help on Python coding. Tyson Waldo, Kate Ramsden, and Gus Seixas contributed to generating, editing, and attributing hydrograpy. The 2016 Skagit LiDAR was obtained through a cooperative agreement among the Washington DNR, Swinomish Tribe, Skagit County, and the USGS 3DEP program. Other LiDAR provided by the USGS Volcano Observatory and the NOAA Coastal

References Cited

Abbe, T.B., and D.R. Montgomery. 1996. Large woody debris jams, channel hydraulics and habitat formation in large rivers. Regulated Rivers 12: 201-221.

Andersen, H.E., R.J. McGaughey, W.W. Carson, S.E. Reutebuch, B. Mercer, and J. Allan. 2002?. A comparison of forest canopy models derived from lidar and insar

data in a pacific northwest conifer forest. International Archives of Photogrammetry and Remote Sensing, 34(3): 211.217.

Andersen, H.E., S.E. Reutebuch, and R.J. McGaughey. 2006. A rigorous assessment of tree height measurements obtained using airborne lidar and conventional field methods. Can J. Remote Sensing. 32(5): 355-366.

Barton, D.R., W.D. Taylor, and R.M. Biette. 1985. Dimensions of riparian buffer strips required to maintain trout habitat in southern Ontario streams. N. Am. Jrn. Fish. Mgmt. 5: 364-378.

Beechie, T.J., and T.H. Sibley. 1997. Relationships between channel characteristics, woody debris, and fish habitat in northwestern Washington streams. Transactions of the American Fisheries Society 126:217-229.

Benda, L.E., P. Bigelow, and T.M Worsley. 2002. Recruitment of wood to streams in old-growth and second-growth redwood forests, northern California, U.S.A. Canadian Journal of Forest Research 32: 1460-1477.

Beschta, R.L., R.E. Bilby, G.W. Brown, L.B. Holtby, and T.D. Hofstra. 1987. Stream temperature and aquatic habitat: fisheries and forestry interactions. *In*: E.O. Salo and T.W. Cundy (Editors), Streamside Management: Forestry and Fishery Interactions. Contrib. No. 57, Institute of Forest Resources, University of Washington, Seattle, WA, pp 191-232.

Bilby, R.E., and J.W. Ward. 1991. Characteristics and function of large woody debris in streams draining old-growth, clear-cut, and second-growth forests in southwestern Washington. Canadian Journal of Fisheries and Aquatic Sciences 48: 2499-2508.

Bilby, R.E., and P.A. Bisson. 1998. Function and distribution of large woody debris. *In* R.J. Naiman and R.E. Bilby [eds.], Ecology and Management of Rivers. Springer-Verlag, New York. Pp 324-346

Bisson, P.A., Bilby, R.E., Bryant, M.D., Dolloff, C.A., Grette, G.B., House, R.A., Murphy, M.L., Koski, K.V. and Sedell, J.R., 1987. Large woody debris in forested streams in the Pacific Northwest: past, present, and future. *In*: E.O. Salo and T.W. Cundy (Editors), Streamside Management: Forestry and Fishery Interactions. Contrib. No. 57, Institute of Forest Resources, University of Washington, Seattle, WA, pp 143-190.

Bode, C. A., M.P. Limm. M.E. Power, J.C. Finley. 2014. Subcanopy solar radiation model: predicting solar radiation across a heavily vegetated landscape using LiDAR and GIS solar radiation models. Remote Sensing of Environment 154: 387-397.

Brazier, J.R., and G.W. Brown. 1973. Buffer strips for stream temperature control. Research Paper 15. Forest Research Laboratory, Oregon State University, Corvallis, Oregon, USA.

Brown, G.W. 1969. Predicting temperatures of small streams. Water Resources Research 5(1): 68-75

Brown, G.W., and J.T. Krygier. 1970. Effects of clear-cutting on stream temperature. Water Resources Research 6(4): 1133-1139

Brown, T.G., and G.F. Hartman. 1988. Contribution of seasonally flooded lands and minor tributaries to the production of coho salmon in Carnation Creek, British Columbia. Trans. Am. Fish. Soc. 117:546-551.

Bustard, D.R., and D.W. Narver. 1975. Aspects of the winter ecology of juvenile coho salmon (*Oncorhynchus kisutch*) and steelhead trout (*Salmo gairdneri*). Journal of the Fisheries Research Board of Canada. 32: 667-680.

Collins, B.D., D.R. Montgomery, K.L. Fetherston, T. B. Abbe. 2012. The floodplain large-wood cycle hypothesis: A mechanism for the physical and biotic structuring of temperate forested alluvial valleys in the North Pacific coastal ecoregion. Geomorphology 139-140: 460-470.

Czarnomski, N.M., D.M. Dreher, J.U. Snyder, J.A. Jones, and F.J. Swanson. 2008. Dynamics of wood in stream networks of the western Cascades Range, Oregon. Canadian Journal of Forest Research 38: 2236-2248.

Fausch, K.D., and T.G. Northcote. 1992. Large woody debris and salmonid habitat in a small coastal British Columbia stream. *Can. J. Fish. Aquat. Sci.* 49: 682-693.

Fullerton, A.H., T.J. Beechie, S.E. Baker, J.E. Hall, K.A. Barnas. 2006. Regional patterns of riparian characteristics in the interior Columbia River basin, Northwestern USA: applications for restoration planning. Landscape Ecology. 21: 1347-1360.

Gregory, S., K. Boyer, and A. M. Gurnell, editors. 2003. The ecology and management of wood in world rivers. American Fisheries Society, Symposium 37, Bethesda, Maryland.

Hall, J.E., Greene, C.M., Stefankiv, O., Anderson, J.H., Timpane-Padgham, B., Beechie, T.J. and Pess, G.R., 2018. Large river habitat complexity and productivity of Puget Sound Chinook salmon. *Plos one*, *13*(11), p.e0205127.

Hofle, B. M. Vetter, N. Pfeifer, G. Mandlburger, and J. Stotter. 2009. Water surface mapping from airborne laser scanning using signal intensity and elevation data. Earth Surface Processes and Landforms 34: 1635-1649

Hyatt, T.L., T.Z. Waldo, and T.J. Beechie. 2004. A watershed-scale assessment of riparian forests, with implications for restoration. *Restoration Ecology* 12(2): 175-183.

Isaak, D. J., Wenger, S. J., Peterson, E. E., Ver Hoef, J. M., Nagel, D. E., Luce, C. H., ... & Chandler, G. L. 2017. The NorWeST summer stream temperature model and scenarios for the western US: A crowd-sourced database and new geospatial tools foster a user community and predict broad climate warming of rivers and streams. *Water Resources Research*, *53*(11), 9181-9205.

Janisch, J.E., S.M. Wondzell, and W.J. Ehinger. 2012. Headwater stream temperature: interpreting response after logging, with and without riparian buffers, Washington, USA. Forest Ecology and Management. 270: 302-313

Johansen, Kasper, Dirk Tiede, Thomas Blaschke, Lara Arroyo, and Stuart Phinn. 2011. Automatic geographic object based mapping of streambed and riparian zone extent from LiDAR data in a temperate rural urban environment, Australia. Remote Sensing (3) 1139-1156. doi:10.3390/rs3061139

Johnson, S.L. 2004. Factors influencing stream temperatures in small streams: substrate effects and a shading experiment. Can. J. Fish. Aquat. Sci. 61: 913-923.

Johnston, N.T., S.A. Bird, D.L. Hogan, and E.A. MacIsaac. 2011. Mechanisms and source distances for the input of large woody debris to forested streams in British Columbia, Canada. Can. J. For. Res. 41: 2231-2246

Kammer, N. M. Olis, C. Veldhuisen, and S. Morris. 2020. Forested tributary stream temperature monitoring in the Skagit Watershed: 2008-2018 results and interpretation. Skagit River System Cooperative. La Conner, WA.

Kasprak, A., F.J. Magilligan, K.H. Nislow, N.P. Snyder. 2012. A LiDAR-derived evaluation of watershed-scale large woody debris sources and recruitment mechanisms: coastal Maine, USA. River Research and Applications 28: 1462-1476.

Lefsky, M.A., Cohen, W.B., Parker, G.G. and Harding, D.J., 2002. Lidar remote sensing for ecosystem studies. *BioScience*, *52*(1), pp.19-30.

Lienkaemper, G.W., and F.J. Swanson. 1987. Dynamics of large woody debris in streams in old-growth Douglas-fir forests. Canadian Journal of Forest Research 17:150-156.

Lunetta, R.S., B.L. Consentino, D.R. Montgomery, E.M. Beamer, and T.J. Beechie. 1997. GIS-based evaluation of salmon habitat in the Pacific Northwest. Photogrammetric Engineering & Remote Sensing **63**: 1219-1229.

May, C.L. and R.E. Gresswell. 2003. Large wood recruitment and redistribution in headwater streams in the southern Oregon Coast Range, U.S.A. Can. J. For. Res. 33: 1352-1362

McDade, M.H., F.J. Swanson, W.A. McKee, J.F. Franklin, and J. Van Sickle. 1990. Source distances for coarse woody debris entering small streams in western Oregon and Washington. Canadian Journal of Forest Research 20: 326-330.

Means, J. E., S.A. Acker, B.J. Fitt, M. Renslow, L. Emerson, and C.J. Hendrix. 2000. Predicting forest stand characteristics with airborne scanning lidar. Photogrammetric Engineering & Remote Sensing 66(11): 1367-1371.

Michez, A. H. Piegay, F. Toromanoff, D. Brogna, S. Bonnet, P. Lejeune, and H. Claessens. 2013. LiDAR derived ecological integrity indicators for riparian zones: application to the Houille river in southern Belgium/Northern France. Ecological Indicators 34: 627-640

Montgomery, D.R., J.M. Buffington, R.D. Smith, K.M. Schmidt, and G. Pess. 1995. Pool spacing in forest channels. Water Resources Research 31(4): 1097-1105.

Montgomery, D.R., T.B. Abbe, J.M. Buffington, N. Phil Peterson, Kevin M. Schmidt, and J.D. Stock. 1996. Distribution of bedrock and alluvial channels in forested mountain drainage basins. Nature 381: 587-589.

Mücke, Werner, and Markus Hollaus. 2011. Modelling light conditions in forests using airborne laser scanning data. Proceedings of the Silvilaser….

Murphy, M.L., and K.V. Koski. 1989. Input and depletion of woody debris in Alaska streams and implications for streamside management. North American Journal of Fisheries Management 9: 427-436.

Naiman, R.J., R.E. Bilby, and P.A. Bisson. 2000. Riparian ecology and management in the Pacific Coastal Rain Forest. BioScience 50(11):996-1011.

Penaluna, Brooke, Jason Dunham, and Heidi Anderson. 2020. Nowhere to hide: the importance of instream cover for stream-living coastal cutthroat trout during seasonal low flow. Ecology of Freshwater Fish (00) 1-14. doi: 10:1111/eff.12581

Pierce, K., Quinn, T.P., Folkerts, K., Miller, J., Samson, K. and Muller, M., 2018. Seven years of development and change within 200'of the shore in Puget Sound. 2018 Salish Sea Ecosystem Conference, Seattle, WA

Pollock, M.M, T.J. Beechie, M. Liermann, and R.E. Bigley. 2009. Stream temperature relationships to forest harvest in western Washington. JAWRA 45(1): 141-156. DOI: 10.1111/j.1752-1688.2008.00266.x

Poole, G.C. and C.H. Berman. 2001. An ecological perspective on in-stream temperature: natural heat dynamics and mechanisms of human-caused thermal degradation. Environmental Management 27(6): 787-802

Poole, G.C., J.A. Stanford, C.A. Frissell, S.W. Running. 2002. Three-dimensional mapping of geomorphic controls on flood-plain hydrology and connectivity from aerial photos. Geomorphology 48: 329-347

Quinn, T., G. Wilhere, and K. Krueger. 2020. Riparian Ecosystems, Volume 1: Science synthesis and management implications.). A Priority Habitat and Species Document of the Washington Department of Fish and Wildlife, Olympia.

Quinn, T., Wilhere, G., and K. Krueger. 2018. Riparian Ecosystems, Volume 1: Science synthesis and management implications. A Priority Habitat and Species Document of the Washington Department of Fish and Wildlife, Olympia.

Reeves, G.H., K.M. Burnett, and E.V. McGarry. 2003. Sources of large wood in the main stem of a fourth-order watershed in coastal Oregon. Can. Jrn. For. Res. 33: 1363-1370

Robison, G.E. and R.L. Beschta. 1990c. Identifying trees in riparian areas that can provide coarse woody debris to streams. Forest Science 36(3) 790-801

Roni, P. and T.P. Quinn. 2001. Density and size of juvenile salmonids in response to placement of large woody debris in western Oregon and Washington. Canadian Journal of Fisheries and Aquatic Sciences 58: 282-292.

Rosenfeld, J. M. Porter, and E. Parkinson. 2000. Habitat factors affecting the abundance and distribution of juvenile cutthroat trout (Oncorhynchus clarki) and coho salmon (Oncorhynchus kisutch). Can. J. Fish. Aquat. Sci. 57: 766-774.

Scheuerell, M.D., C.P. Ruff, J.H. Anderson, and E.M. Beamer. 2020. An integrated population model for estimating the relative effects of natural and anthropogenic factors on a threatened population of steelhead trout. Journal of Applied Ecology 2020(00) 1-11.

Schuett-Hames, Dave, and Greg Stewart. 2019. Changes in stand structure, buffer tree mortality and riparian-associated functions 10 years after timber harvest adjacent to non-fish-bearing perennial streams in western Washington. Cooperative Monitoring Evaluation and Research report CMER #2019.10.22.B. Washington Department of Natural Resources, Olympia, WA

Seixas, Gustav B., Timothy J. Beechie, Caleb Fogel, and Peter M. Kiffney. 2018. Historical and future stream temperature change predicted by a LiDAR-based assessment of riparian condition and channel width. JAWRA 1-18. DOI:10.1111/1752-1688.12655

Skagit River System Cooperative and Washington Department of Fish and Wildlife. 2005. Skagit Chinook Recovery Plan. Skagit River System Cooperative, La Conner, WA. Available at www.skagitcoop.org/.

Steinblums, I.J., H.A. Froehlich, and J.K. Lyons. 1984. Designing stable buffer strips for stream protection. Journal of Forestry 82: 49-52.

Swanson F.J. and G.W. Lienkaemper. 1978. Physical consequences of large organic debris in Pacific Northwest streams. GTR-PNW-69. Pacific Northwest Range and Experiment Station, Portland, OR.

Tompalski, P. N.C. Coops, J.C. White, M.A. Wulder, and A. Yuill. 2017. Characterizing streams and riparian areas with airborne laser scanning data. Remote Sensing of Environment 192: 73-86

Tschaplinski, P.J., and G.F. Hartman, 1983. Winter distribution of juvenile coho salmon (*Oncorhynchus kisutch*) before and after logging in Carnation Creek, British Columbia, and some implications for overwinter survival. Canadian Journal of Fisheries and Aquatic Science 40: 452-461.

Van Sickle, J. and S.V. Gregory. 1990. Modeling inputs of large woody debris to streams from falling trees. Canadian Journal of Forest Research. 20: 1593-1601

Wasser, L., L. Chasmer, R. Day, and A. Taylor. 2015. Quantifying land use effects on forested riparian buffer vegetation structure using LiDAR data. Ecosphere 6(1):10. DOI 10.1890/ES14-00204.1

Wasser, L., R. Day, L. Chasmer, A. Taylor. 2013. Influence of vegetation structure on Lidar-derived canopy height and fractional cover in forested riparian buffers during leaf-off and leaf-on conditions. PLoS ONE 8(1): e54776. doi: 10.1371/journal.pone.0054776.